

# First clinical experience using a novel high-resolution electroanatomical mapping system for left atrial ablation procedures

Christian Sohns<sup>1</sup> · Ardan M. Saguner<sup>1</sup> · Christine Lemes<sup>1</sup> · Francesco Santoro<sup>1</sup> ·  
Shibu Mathew<sup>1</sup> · Christian Heeger<sup>1</sup> · Bruno Reißmann<sup>1</sup> · Tilman Maurer<sup>1</sup> ·  
Johannes Riedl<sup>1</sup> · Thomas Fink<sup>1</sup> · Kentaro Hayashi<sup>1</sup> · Feifan Ouyang<sup>1</sup> ·  
Karl-Heinz Kuck<sup>1</sup> · Andreas Metzner<sup>1</sup>

Received: 22 February 2016 / Accepted: 6 June 2016 / Published online: 11 June 2016  
© Springer-Verlag Berlin Heidelberg 2016

## Abstract

**Background** The Rhythmia mapping system was recently launched and allows for rapid ultra-high-resolution electroanatomical mapping. We evaluated the feasibility, acute efficacy and safety of this novel system for ablation of atrial fibrillation (AF) and left atrial (LA) tachycardia (AT).

**Methods and results** A total of 35 consecutive patients (age  $64.3 \pm 8.6$  years, LA diameter  $44.4 \pm 5.8$  mm) underwent catheter ablation for AF and/or AT. All procedures were performed using Rhythmia in conjunction with the Orion mini-basket catheter. Pulmonary vein isolation (PVI) and linear lesions were performed applying radiofrequency (RF) energy. PVI was confirmed by presence of entrance and exit block using the mini-basket catheter. In addition, pacing maneuvers assessed bidirectional conduction block across linear lesions. Procedure duration was  $110.3 \pm 33$  min, fast acquisition mapping (FAM) time was  $19 \pm 9$  min. A mean number of  $10165 \pm 5904$  mapping points were acquired during the initial map and  $6379 \pm 3191$  for a remap. A total number of  $31 \pm 15$  RF applications were delivered within  $45 \pm 22$  min. Total fluoroscopy time was  $21 \pm 5$ ,  $5 \pm 2$  min were used for FAM. We observed a significant learning curve for mapping duration ( $p = 0.01$ ). Complications included pericardial tamponade ( $n = 1$ ), transient

air embolism in the right coronary artery ( $n = 1$ ), and mild groin hematoma ( $n = 2$ ).

**Conclusions** The present study is the largest to describe experience of LA ablation procedures using Rhythmia. PVI was achieved in all patients. Applying this ultra high-resolution electroanatomical mapping system under routine conditions leads to a high level of confidence. More data will be mandatory before final conclusions can be drawn.

**Keywords** Atrial fibrillation · Electroanatomical mapping · Pulmonary vein isolation

## Introduction

Pulmonary vein isolation (PVI) is an effective treatment option in patients suffering from paroxysmal (PAF) and short-standing persistent atrial fibrillation (PERS). Freedom from PAF after PVI is reported from 56 to 89 % after 1 year [1]. However, multiple procedures can be mandatory due to recurrence of atrial fibrillation (AF) or atrial tachycardia (AT). Reconnection of previously isolated pulmonary veins (PV) and conduction across previously complete linear ablation lesions are frequently observed at repeat ablation procedures [2, 3], and might explain the modest success rates [4].

Today, several electroanatomical mapping (EAM) systems utilizing various technologies are used in clinical routine to facilitate mapping and ablation. Most of the established EAM use point-by-point acquisition of electrograms from a roving catheter with or without multi-electrode mapping capability, and usually require manual annotation [5, 6]. Recently, a novel mapping system (Rhythmia, Boston Scientific, Cambridge, MA, USA) became commercially available and allows for rapid and

---

C. Sohns and A. M. Saguner contributed equally to this work.

✉ Christian Sohns  
c.sohns@asklepios.com

<sup>1</sup> Department of Cardiology, Asklepios Klinik St. Georg,  
Lohmühlenstraße 5, 20099 Hamburg, Germany

ultra high-resolution EAM and activation mapping. This system is paired with a mini-basket catheter consisting of 64 electrodes (IntellaMap Orion, Boston Scientific, Cambridge, MA, USA), which allows for simultaneous acquisition and automatical annotation of thousands points. Rhythmia has demonstrated its ability to rapidly obtain high-resolution maps in animal models with no need for additional manual annotation [7, 8]. Recently, two small clinical studies reported that the Rhythmia system in conjunction with the Orion catheter allows for determination of successful PVI, and may be feasible for ablation of complex atrial and ventricular arrhythmias [9, 10]. However, since these previous studies investigated a limited number of patients and heterogeneous arrhythmias, we sought to determine the acute procedural efficacy and safety of this new system in a larger patient cohort with atrial fibrillation (AF) and left atrial tachycardia (AT).

## Methods

### Patients

In this single-center study, the first 35 consecutive LA ablation procedures using Rhythmia in conjunction with the Orion mini-basket catheter were analyzed. All clinical, imaging, and procedural data were recorded. Written informed consent was obtained from each patient prior to the procedure. The current study is a retrospective analysis and was approved by the local ethics committee (WF-07/16 Ärztekammer, Hamburg, Germany).

### Procedural setup

A transoesophageal echocardiogram was performed prior to ablation to rule out LA thrombus formation. AF as well as AT ablation were performed on uninterrupted oral vitamin K anticoagulants with an INR of 2.0–3.0 at the day of the procedure. If a non-vitamin K anticoagulant was used, this was discontinued 24 h before ablation. Catheter ablation was performed under deep sedation with continuous infusion of propofol. A 6-F catheter was inserted into the distal coronary sinus via the right femoral vein to achieve a stable position. Stable positioning was facilitated by introducing the 6-F catheter via a long 8.5 F sheath placed in the proximal coronary sinus (SL1, St. Jude Medical Inc, St. Paul, MN, USA). Placement of two additional 8.5 F SL1 sheaths in the LA using the modified Brockenbrough technique was performed as previously described in detail [11]. After transseptal puncture, intravenous heparin was administered, targeting an activated clotting time (ACT) of >300 s, and monitored every

30 min throughout the procedure with adjustment to the heparin dosage according to the ACT.

### Mapping system and mini basket multi-electrode catheter

The Rhythmia mapping system and the Orion mini-basket catheter were previously described [9, 10]. Briefly, Rhythmia is a rapid high-resolution three-dimensional (3D) EAM that uses a hybrid location technology combining magnetic and impedance location. The magnetic field is generated by a localization generator positioned under the patient, and is capable of locating the magnetically tracked mini-basket catheter with an accuracy of  $\leq 1$  mm. The impedance location technology (accuracy of  $\leq 2$  mm) is used to track catheters that are not equipped with a magnetic sensor, e.g., ablation catheters and diagnostic coronary sinus (CS) catheters in this study. The system then maps the impedance field measurements to the magnetic location coordinates and creates an impedance field map. This map is used to enhance the accuracy of the impedance location. The Orion catheter is a bidirectional deflectable, multielectrode, mini-basket mapping catheter with a maximum shaft diameter of 8.5 F. It was advanced into the LA via an 8.5 F SL1 sheath. This basket catheter can acquire points at variable degrees of deployment from undeployed (3 mm) to fully deployed (22 mm).

### Map acquisition

The mini-basket catheter was gently and slowly manipulated inside the LA, pulmonary veins (PV) and left atrial appendage (LAA), and automatically acquired points with every accepted beat. Criteria used for beat acceptance were (a) stable cycle length (CL), (b) stable timing difference between two reference electrodes, (c) respiration gating, (d) stable catheter location (e) stability of catheter signal compared to adjacent points and (f) tracking quality.

### Voltage and activation maps

The mapping window setup is automatically generated. Therefore, the system calculates the mean CL of the underlying rhythm over 10 s and consequently sets 100 % of CL equally before and after the timing reference electrode. The final maps visualize the activation propagation. For bipolar time maps, the timing of the electrodes was based on time difference between the maximum amplitude of the bipolar electrogram and the first reference CS electrode (timing reference). For electrograms with more than one potential, the system selects the potential that best matches the timing of the surrounding electrograms. For

unipolar time maps, the timing was based on the most negative  $dV/dT$  around the timing of the max bipolar signal. The bipolar and unipolar voltage maps were based on the difference between the maximum and minimum peak of the signal that is automatically annotated. For the LA, noise level and complete electrical silence were considered as  $<0.01$  mV and annotated in gray color, low voltage areas were generally detected between 0.01 and 0.5 mV ( $<0.2$  mV assumed to be scar, annotated in red). Except for patients presenting with AT, all remaining maps and remaps were acquired during either sinus rhythm, or if sinus rhythm was slow or unstable during atrial pacing from the CS. In patients presenting with AF as the initial rhythm, electrical cardioversion was performed after transseptal puncture prior to mapping of the LA, which was achieved in all patients.

### Chamber geometry

The geometry of the LA, LAA, and PVs was gradually acquired with every accepted beat based on the location of the outermost electrodes of the mini-basket catheter. To access the PVs and LAA, the Orion catheter was inserted in an undeployed mode, then deployed within the PVs and LAA, and slowly pulled back. In all cases, the system was programmed to select and include only electrograms up to 2–5 mm from the surface geometry.

### Ablation procedure

Ablation was performed with an open-irrigated catheter (3.5 mm tip ThermoCool Celsius, Biosense Webster, Diamond Bar, CA, USA or 4 mm Blazer, Boston Scientific, Cambridge, MA, USA). After reconstruction of the LA, each PV ostium was identified by selective PV angiography and tagged on the 3D map. Afterwards, wide-area circumferential ablation (WACA) of the ipsilateral PVs was performed aiming for PVI, while the mini-basket catheter was placed in the respective PVs in a proximal position (Figs. 1, 2). An anterior line from the mitral annulus to the right superior PV was performed in case of perimitral flutter (Figs. 3, 4, 5). Irrigated radiofrequency (RF) current energy was delivered as previously described, targeting a maximum temperature of 43 °C, a maximal power level of 40 W, and an infusion rate of 17–25 mL/min. Along the posterior wall, the maximum power was limited to 30 W. The procedural end points were defined as follows: (a) for PVI: the presence of entrance and exit block within the PVs using the mini-basket catheter, (b) for AT: PVI + termination and/or non-inducibility of AT with atrial burst pacing (minimal cycle length 200 ms), and bidirectional block along LA lines.

### Statistical analysis

Statistical analysis was performed using SPSS for Windows (Version 19.0, SPSS Inc., Chicago, IL, USA). Continuous variables are expressed as mean  $\pm$  standard deviation or as median with inter-quartile range, as appropriate. Normally distributed data were compared using the unpaired Student's *t* test. A *p* value of  $<0.05$  was considered as statistically significant.

### Results

We studied 35 consecutive patients, aged  $64.3 \pm 8.6$  years, 15/35 (43 %) male. A total of 21 patients presented with PAF, 8 patients with PERS, and 6 patients with left AT. The clinical baseline characteristics of the entire study population are presented in Table 1. A total number of 56 high-resolution maps were acquired using the mini-basket mapping catheter.

### Procedural data

Normal PV anatomy was present in all patients. A total of 140 PVs were identified and successfully isolated. PVI was visualized by the mini-basket catheter (Figs. 1, 2). Average procedure duration (time from venous puncture to removal of all sheaths) was  $110.3 \pm 33$  min., mapping time was  $19 \pm 9$  min. A mean number of  $10,165 \pm 5904$  mapping points were acquired during the initial map, and  $6379 \pm 3191$  for remaps (performed in 21/35 (60 %) patients). A mean total number of  $31 \pm 15$  RF applications were delivered within  $45 \pm 22$  min. Mean total fluoroscopy time was  $21 \pm 5$ ,  $5 \pm 2$  min were used for mapping of the LA/PVs. Correction of automatic annotation was not necessary to reach procedural endpoints. Procedural data is summarized in Table 2.

### Safety and complications

The mini-basket catheter was flushed and inserted to the cardiac chambers after an ACT  $>300$  s was achieved, and maintained with boluses of intravenous heparin. We observed no embolic complications, including stroke or systemic embolism. All catheters were checked and found to be free from any visible thrombus formation at the end of the ablation procedure. One patient developed pericardial tamponade 3 h after the procedure, which could be successfully drained (venous blood) without sequelae. Tamponade was judged as probably unrelated to the basket catheter. As minor complications a transient air embolism ( $n = 1$ ) in the right coronary artery resolving sponta-

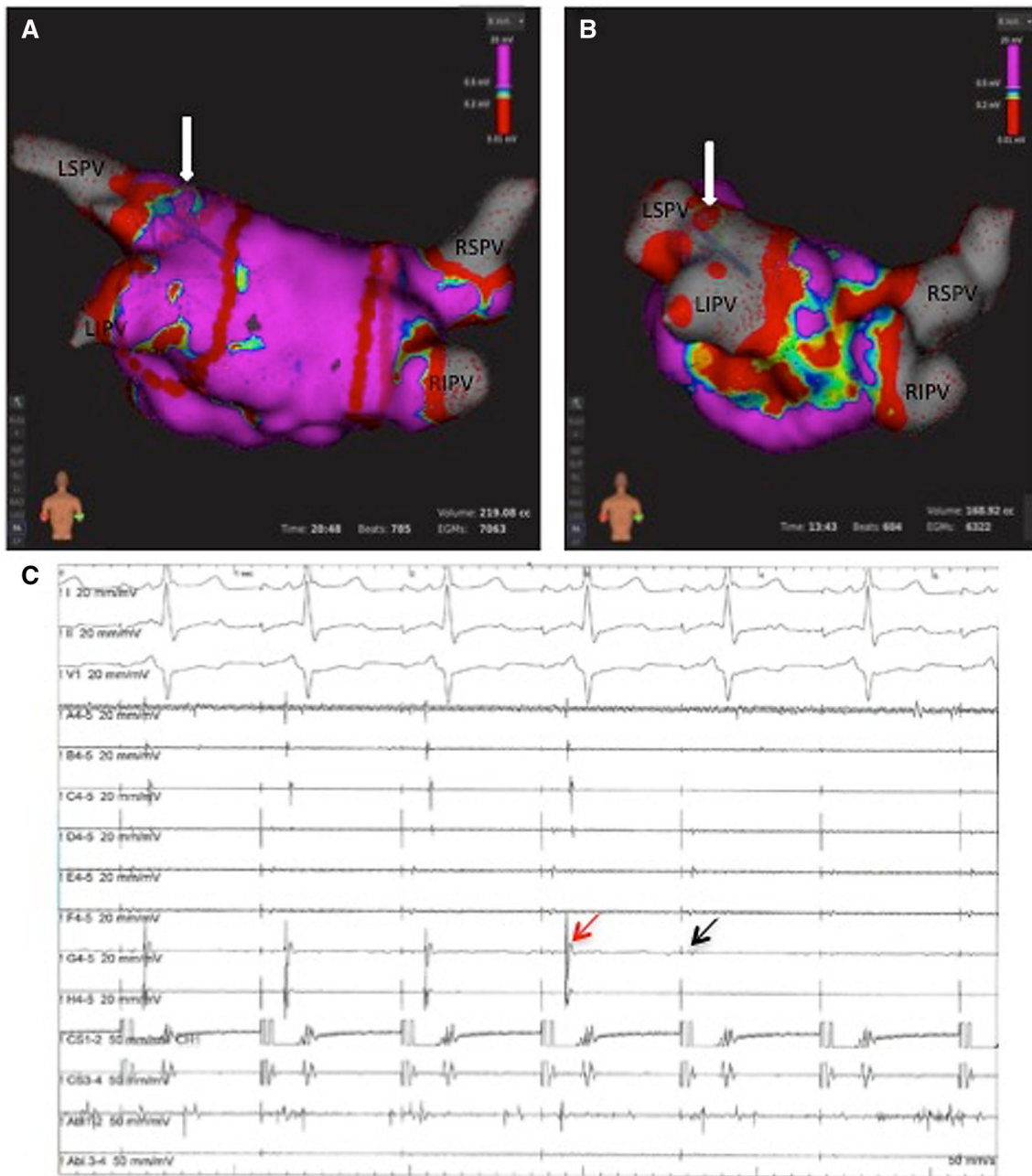


**Fig. 1** The upper two panels show a 3D reconstruction of the left atrium (LA) and pulmonary veins (PV) during sinus rhythm in a postero-anterior (PA) view. **a** Visualizes the LA myocardium with normal bipolar voltages (>0.5 mV, purple) and the PVs with low voltage (other colors than purple) in this patient with paroxysmal atrial fibrillation. Gray zones indicate complete electrical silence (<0.01 mV). The mini-basket catheter (white arrow) is placed within the left superior PV (LSPV). Wide-area circumferential ablation (WACA) was performed around the ipsilateral PVs (ablation points marked with red dots). Time indicates mapping time in min/sec, EGMs indicates number of electrograms acquired with the basket catheter. **b** A remap of the LA and PVs during sinus rhythm after PV isolation. Note that previously purple areas inside the ablation circle

now appear in gray or red color (red far field signals (<0.2 mV) from the LA/LAA, see also black arrow in c), indicating successful PV isolation (entrance block). **c** The surface ECG (top lead I, II, and V1) and intracardiac electrograms (bottom) during pacing from the distal electrode of the coronary sinus catheter (CS 1–2). Electrical isolation of the LSPV (A4–5 to H4–5: bipolar electrograms from the equatorial electrodes of the basket catheter) is visualized during application of radiofrequency current with the ablation catheter (Abl 1–2; red arrow shows PV spike, black arrow shows atrial far field potential). Abl 3–4 proximal electrodes of the ablation catheter, CS 3–4 proximal coronary sinus electrodes, RSPV right superior PV, RIPV right inferior PV

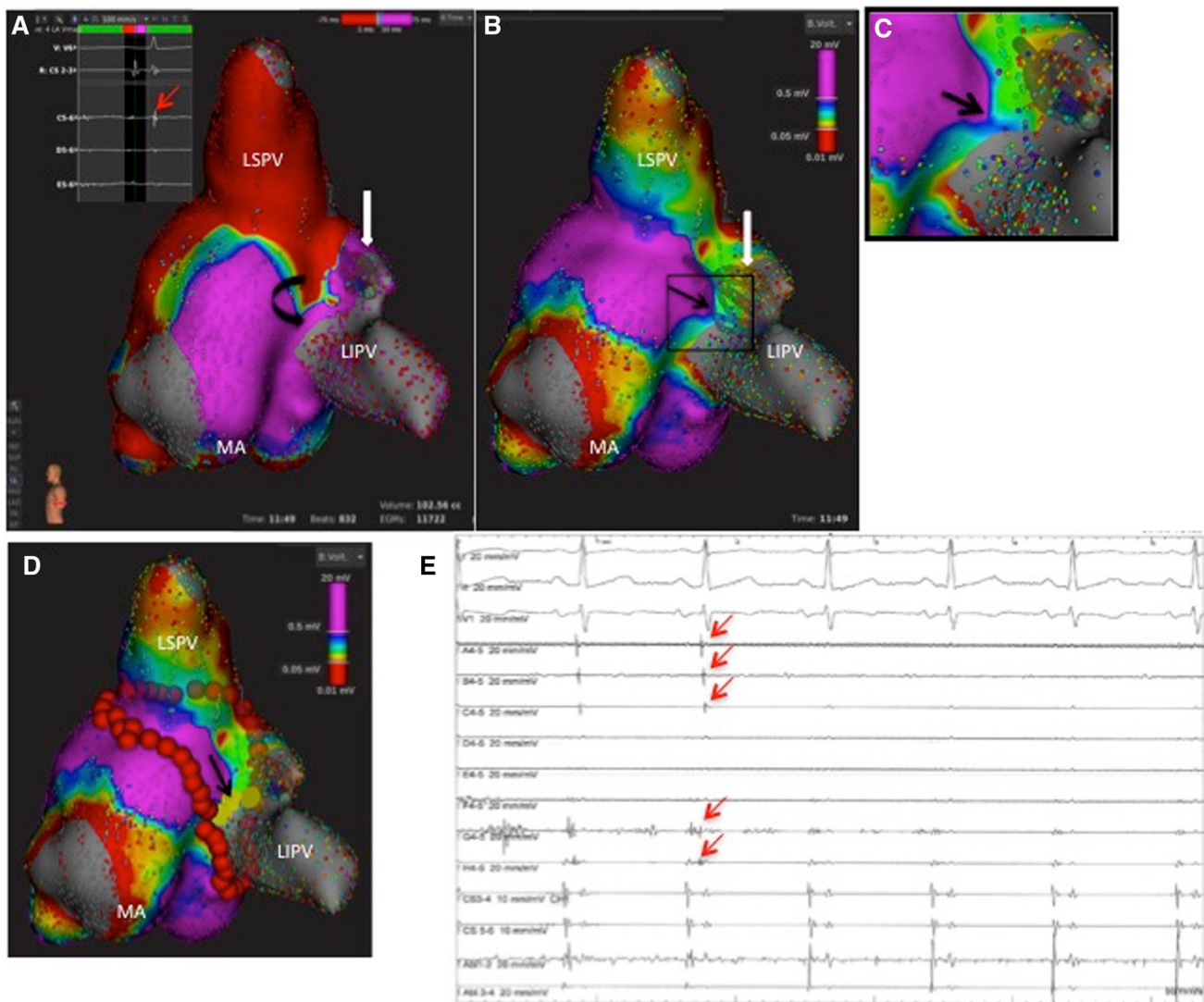


**Fig. 2** The upper two panels show a 3D reconstruction of the left atrium (LA) and pulmonary veins (PV) during sinus rhythm in the left lateral (LL) view after wide-area circumferential ablation (WACA) of the left PVs (LSPV left superior PV, LIPV left inferior PV). **a** An activation map (remap) of the LA during sinus rhythm after WACA. Of note, the superior branch of the LIPV shows late activation (purple area indicated by curved black arrow) during sinus rhythm corresponding to a borderline bipolar voltage area [**b**, black arrow, and **c** (enlarged black box from **b**)]. White arrows indicate position of basket catheter. **d** Rhythmia correctly identified the gap in the

ablation line (red points). The LIPV was isolated in this area (yellow points marked by black arrow). **e** The surface ECG (top lead I, II, and V1) and intracardiac electrograms (bottom) during sinus rhythm. Electrical isolation of the LIPV (A4–5 to H4–5: bipolar electrograms from the equatorial electrodes of the basket catheter; red arrows show PV spike) is visualized during application of radiofrequency current with the ablation catheter (Abl 1–2). Abl 3–4 proximal electrodes of the ablation catheter, CS 3–6 proximal coronary sinus electrodes, MA mitral annulus

neously after 6 min, and mild groin hematoma ( $n = 2$ ) were noted. Once placed and fully deployed inside the LA, the basket catheter never dislodged into the RA.

### Accuracy of maps

The 56 acquired maps showed highly detailed endocardial electrical activation and voltage. Manual re-annotation of automatically acquired mapping points was not necessary

to reach procedural endpoints in this study. PVs, LAA, atrial septum and LA anterior wall were reached and mapped with the mini-basket catheter without the use of a steerable sheath. Of note, all LA sides required for successful ablation were reached using the mini-basket catheter, although we cannot exclude having missed some small parts in the LAA and mitral annulus, since we do not routinely perform computer tomography or magnetic resonance imaging of the LA prior ablation. Yet, accuracy of

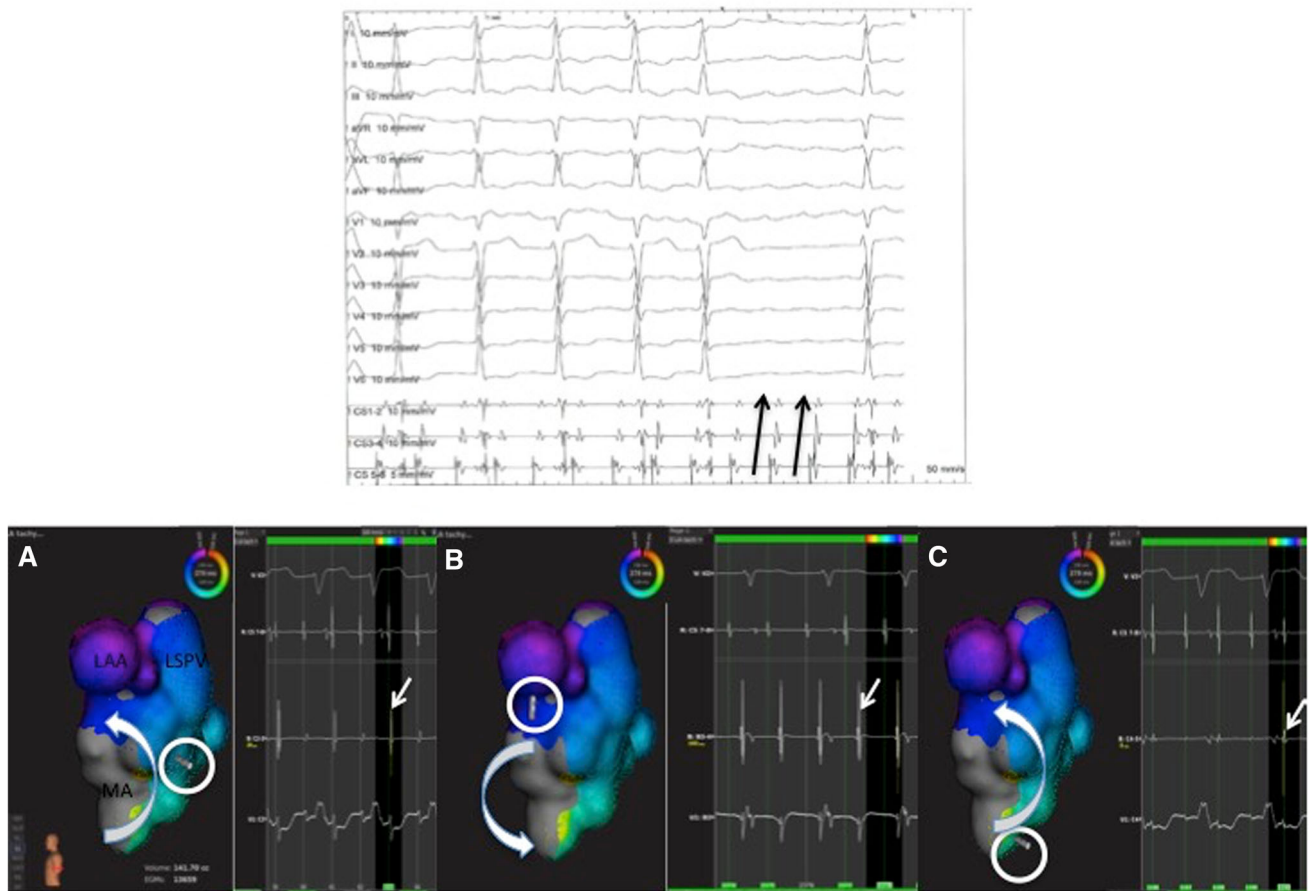


**Fig. 3** Upper panel 12-lead surface ECG and intracardiac electrograms [coronary sinus (CS) catheter] suggest counter-clockwise perimitral LA flutter with a cycle length of 280 ms (CS activation from proximal (CS 5/6) to distal (CS 1–2), *black arrows*) with variable atrioventricular conduction. Lower panel LA electrical propagation is visualized during perimitral flutter (**a–c**; left lateral view). The rowing probe (*white circle*) shows mapping points in the

LA around the mitral annulus (MA), in proximity to the left atrial appendage (LAA) and left superior pulmonary vein (LSPV) obtained by the mini-basket catheter during perimitral flutter. Local activation on the mini-basket catheter (bipolar (**b**), *white arrows*) suggests counter-clockwise perimitral LA flutter (*white curved arrow*). U1 unipolar recordings

LA anatomy was verified by concomitant LA angiographies, additional 3D mapping with the ablation catheter, and careful evaluation of electrograms. All PVs except one (99.3 %) could be intubated with the Orion catheter. One right inferior PV could not be intubated due to a rather posterior transseptal puncture side. The anatomy of this respective PV was reconstructed using the ablation catheter.

The 3D visualization of the mini-basket catheter and the ablation catheter in the EAM well corresponded to fluoroscopic findings, and were internally consistent in the majority of cases. Tracking accuracy was determined comparing the location of the ablation and mini-basket catheter from EAM with selective pulmonary angiography and fluoroscopy throughout the ablation procedure. Tracking accuracy was generally  $\leq 2$  mm. However, in five patients we observed a relevant anatomical map shift

verified by the fluoroscopic location of the catheters requiring a re-map. These map shifts occurred during our very first experience with the system. After placing the reference catheter very distally within the CS, using a long SL-1 sheath if necessary, and avoiding—even small dislodgements of the reference catheter—the problem of relevant map shifts did not re-occur. Distal placement of the CS catheter is routinely performed in our center, but the SL-1 sheath was used in order to ensure accuracy of the Rhythmia system.

**Mapping of specific arrhythmias**

Pulmonary vein isolation applying WACA and simultaneous activation/voltage mapping of the LA with the Orion catheter during sinus rhythm or CS pacing was performed in all patients with PAF ( $n = 21$ ) and PERS ( $n = 8$ ). After



**Fig. 4** *Left panel* (left anterior oblique view, LAO): due to extensive scarring of the left atrial anterior wall (bipolar voltage map, scar  $<0.2\text{ mV}$  displayed in red color), an anterior left atrial ablation line was placed from the superior aspect of the mitral annulus (MA) to the right superior pulmonary vein (RSPV; red dots ablation lesions), LAA left atrial appendage. *Right panel: Top surface ECG* (lead I, II, and

V1) and *bottom* intracardiac electrograms indicating deceleration (from 335 to 370 ms) of counter-clockwise perimitral flutter and finally termination (red arrow) during placement of the anterior ablation line with the ablation catheter (Abl 1–2), black arrow indicates sinus rhythm. CS 1–10 coronary sinus electrodes (CS 1/2 distal, CS 9/10 proximal)

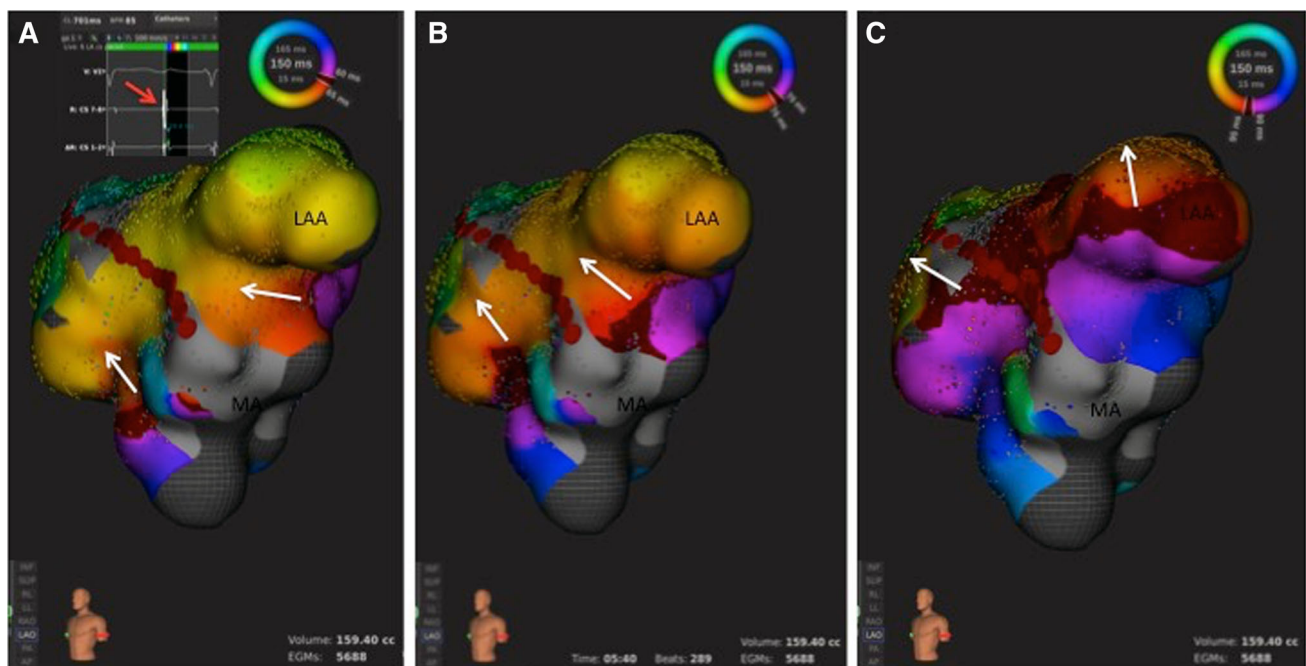


**Fig. 5** Example of electrical propagation in the LA (white arrows, left anterior oblique view) during pacing from the proximal coronary sinus (red arrow) after block of the anterior left atrial ablation line

(red dots). There is no conduction gap within the line, the anterior and posterior LA are activated in parallel, and both activation fronts (white arrows) do not cross the ablation line

ablation, a remap was performed in 21 patients (60 % of all procedures), predominantly to visualize PVI ( $n = 8$ ) (Figs. 1, 2) or to confirm that an atrial ablation line was blocked in patients with previous sustained AT ( $n = 3$ ) (Figs. 3, 4, 5). These remaps were acquired in  $9.4 \pm 4.7$  min, consisting of  $6509 \pm 3980$  points. In all

but two patients the remaps during sinus rhythm showed bipolar voltages  $<0.2\text{ mV}$  within the PVs and PV-LA junction, well corresponding to entrance block on the basket catheter (Figs. 1, 2). In the other two patients, the remap and signals on the basket catheter indicated a conduction gap into the PVs. In one patient, the bipolar

**Table 1** Baseline patient characteristics

Parameter	Patients ( <i>n</i> = 35)
Age	64.3 ± 8.6
Sex: man, <i>n</i> (%)	18 (51)
Paroxysmal AF, <i>n</i> (%)	21 (63)
Duration of the arrhythmia (months)	26 ± 32
Hypertension, <i>n</i> (%)	18 (51)
Diabetes, <i>n</i> (%)	3 (9)
Coronary artery disease, <i>n</i> (%)	5 (15)
History of TIA/stroke	1 (3)
Left ventricular ejection fraction (%)	
Mean ± SD	59 ± 5
Range	47–65
Left atrial diameter (mm)	
Mean ± SD	44.4 ± 5.8
Range	30–55
CHA <sub>2</sub> DS <sub>2</sub> -VASc Score	
Mean ± SD	2 ± 1
Range	0–4
Implanted device, <i>n</i> (%)	1 (3)
EHRA-Score	
Mean ± SD	2 ± 1
Range	2–4
Oral anticoagulation	
Warfarin	10 (30)
NOAC	25 (70)
Valvular heart disease >2°	1 (3)

threshold for scar was reduced from 0.2 to 0.05 mV to facilitate the identification of gaps after initial WACA without direct PVI (Fig. 2).

Six macro re-entry ATs were mapped and in all cases, the novel system annotated 100 % of the CL correctly. Five patients suffered from perimitral AT and one patient presented with a LA roof dependent AT. In this context, Rhythmia allowed visualization of counter-clockwise perimitral flutter in one patient, in whom the LA propagation map comprising 5739 points was acquired within 5.4 min (Fig. 3). Due to extensive scarring of the LA anterior wall, an anterior LA line from the anterior mitral annulus to the right superior PV was placed by slowing down and finally terminating the AT (Fig. 4).

### Learning curve analysis

We divided the 35 patients into two groups in order to perform a learning-curve analysis with particular focus on procedural data between the first 18 and the following 17

**Table 2** Procedural data

Parameter	Procedures ( <i>n</i> = 35)
Type of ablation procedure	
Paroxysmal AF	21
Persistent AF	8
Atrial tachycardia	6
FAM mapping time for the initial map (min)	19 ± 9
Mapping points for the initial map ( <i>n</i> )	10,165 ± 5904
Remap ( <i>n</i> )	21
Mapping points for the remap ( <i>n</i> )	6379 ± 3191
Total ablation time (min)	45 ± 22
Total number of RF applications ( <i>n</i> )	31 ± 15
Total procedure time (min)	110.3 ± 33
All PVs isolated (%)	100
Total number of isolated pulmonary veins ( <i>n</i> )	140
Normal pulmonary vein anatomy (%)	100
Contrast agent (ml)	91.5 ± 21
Mean fluoroscopy time (min)	21 ± 5
Fluoroscopy time for the map (min)	5 ± 2
Cumulative radiation dose (Gy cm <sup>2</sup> )	1691.5 ± 824.7
Minor complications	3
Major complications	1

patients. There were no significant differences regarding patients' characteristics and the type of ablation procedure between the two cohorts. There was a significant reduction of mapping duration using the basket catheter (28 ± 10 vs. 15 ± 7 min; *p* = 0.01), and total procedure time (119 ± 35 vs. 97 ± 25 min; *p* = 0.04), whereas no significant differences were observed for total ablation time (*p* = 0.33), total fluoroscopy time (*p* = 0.84), and cumulative radiation dose (*p* = 0.71).

### Discussion

To the best of our knowledge, this is the largest study evaluating the feasibility, acute efficacy and safety of Rhythmia, a novel high-resolution electroanatomical mapping system, for PVI and ablation of left AT. This analysis has three major findings. First, Rhythmia in conjunction with the Orion catheter allows for rapid and accurate generation of high-density propagation and voltage maps of the LA. Second, this mapping system proved to be effective and safe for PVI and ablation of LA tachycardia. Third, we were able to demonstrate a significant learning curve for manipulating the mini-basket catheter within the LA, thereby reducing mapping and overall procedure time.



## Procedural data

Our fluoroscopy times were higher compared to some previous studies since we routinely perform selective PV angiography to annotate the PV-LA junction in the 3D mapping system. Yet, the mean procedure duration and fluoroscopy time of this study did not significantly differ from previous LA ablation data reported from our own group [11]. During the very first ablation procedures we observed a relevant anatomical shift in five patients. As a consequence, a re-map was performed using the mini-basket or ablation catheter. Instability of the diagnostic reference catheter placed within the CS and responsible for accurate impedance tracking of the ablation catheter, has been reported as a potential reason for the map shift [12]. The re-maps prolonged procedure duration and fluoroscopy times by no more than 30/5 min, respectively. In this context, the hybrid location technology of Rhythmia allows the utilization of diagnostic and therapeutic catheters without magnetic sensors including such from other providers. However, potential disadvantages constitute the lower tracking accuracy of impedance based tracking ( $\leq 2$  mm) as compared to magnetic tracking ( $\leq 1$  mm), as well as the predisposition for relevant map shifts depending on the motion and dislocation of the diagnostic reference catheter. In this study, we observed no more relevant map shifts after placing the reference catheter very distally within the CS.

## Generation of maps

Our initial data demonstrates that Rhythmia can be used in a routine clinical setup. In addition, the basket catheter can safely be manipulated within the atria, and does not require any additional stiff wire or balloon to be deployed [13, 14]. All anatomical regions were reached without the need for a steerable sheath. The PVs and LAA were intubated in an undeployed mode, whereas the LA anterior wall and septal part could be reached in the deployed mode. Irrespective of this observation, a long steerable sheath may be useful in very dilated atria or in patients with challenging anatomy like congenital heart disease [15].

Using the established 3D EAM, the acquisition of even some hundred points can be time-consuming and a manual annotation is often required. The Orion catheter features 64 closely spaced electrodes with a low noise level of generated contact electrograms. In conjunction with Rhythmia and its specific algorithm for point acquisition and annotation, several thousand points were acquired during sinus rhythm, pacing from the CS or during AT with high accuracy. At the same time, all points were automatically annotated by the system in about 20 min with a mean fluoroscopy time of  $5 \pm 2$  min (Table 2). Furthermore, there was no need for manual re-annotation of

automatically annotated points to reach our procedural endpoints, which is in line with previous data [7, 10].

## Mapping of specific arrhythmias

In the current study, the Rhythmia system was used to evaluate its acute procedural efficacy, safety, and potential limitations in the ablation of LA arrhythmias. Our data demonstrate that Rhythmia in conjunction with the mini-basket catheter can reliably visualize PVI, detect gaps after WACA, and visualize electrical propagation of atrial macroreentrant tachycardia, corroborating previous results from animal and human studies [7, 9, 10, 16].

In this context, Anter et al. [9] have shown that the Orion catheter underestimates PVI in comparison to a standard circumferential spiral mapping catheter. This was explained by the potential issue that the mini-basket catheter is very sensitive for picking up electrical signals due to its 64 electrodes. In our study, we evaluated the ability to confirm PVI using the Orion catheter, as assessment of PVI did not pose any challenge with our local approach. Furthermore, focused ablation on the site of the revealed gap from atrial voltage mapping after incomplete WACA led to immediate PVI [17]. In case of an AT, the atrial voltage assisted to decide on further linear lesions, based on highly detailed information of LA voltage and scarring. As can be appreciated from Figs. 1 and 4, patients with PAF and PERS AF/AT had variable amounts of LA low voltage, which was expected, and in line with previous studies on older 3D mapping systems. Patients with PAF presented with normal LA voltages ( $>0.5$  mV). In patients with AT, Rhythmia was able to visualize area of low voltage/scar, guiding AT ablation in these patients. As can be depicted from Fig. 4, this patient with perimitral flutter had extensive scarring of the anterior LA wall, so the detailed voltage map was very helpful to guide ablation. In this case, we decided to deploy an anterior ablation line from the anterior aspect of the mitral annulus to the right superior PV, instead of deploying a posterior mitral-isthmus line, since it is easier to block the anterior line in case of extensive anterior scarring than the mitral isthmus. Of note, without high-resolution mapping LA macro re-entrant tachycardia with multiple circuits may have been misinterpreted as AF in one patient. However, it may be necessary to decrease bipolar voltage cut-offs for visualizing scar tissue for an improved understanding of the substrate (Fig. 2), since the electrical signals recorded from the basket catheter have a very low noise level of  $<0.01$  mV. Thus, the system may improve the differentiation of complete electrical silence, e.g., within the very distal PVs, from areas with some remaining myocardial fibers within scar tissue. Yet, differentiation between far field signals and local PV spikes can sometimes be challenging with the

Rhythmia system, particularly for the superior PVs. Thus, in our study electrical isolation of PV was always confirmed by routine measures such as demonstration of entrance block on the mini-basket catheter during sinus rhythm and pacing from the distal CS/LAA, as well as exit block by pacing from the PVs with local capture of PV myocardium. In fact, remaps after electrical isolation sometimes showed far field potentials as can be appreciated from Fig. 1, particularly in the left superior PV, which is dependent on the anatomy of the PV-LA junction and proximity of the left PVs and LAA. However, these far field signals did not display bipolar voltages  $>0.2$  mV, yielding a color code of gray ( $<0.01$  mV) or red ( $<0.2$  mV). Activation maps after PVI were rarely required, but as can be appreciated from Fig. 2 the activation re-map in this patient during sinus rhythm showed red signals (early activation) in the left superior PV, although this PV was isolated by standard measures. When electrical signals in the left superior PV during this activation re-map were analyzed, we verified that these signals were early and preceded atrial signals in the CS, reflecting far field signals from the LA/LAA. Thus, we believe that particularly for the superior PVs in case of any doubt, after PVI it may be important to manually proof local signals and automated annotation with the rowing probe.

### Learning curve

To perform a learning-curve analysis for using Rhythmia in conjunction with the Orion catheter, we observed differences in procedural data between the first 18 and the following 17 patients. Although there were no significant differences regarding patient characteristics and the type of ablation procedure between the two cohorts, we observed a significant shortening of mapping duration, and total procedure time, which is in line with previous data [18–20]. Shorter total procedure times were mostly related to shorter mapping times with the mini-basket catheter and avoidance of relevant anatomical shifts necessitating remaps, since other procedural parameters did not significantly differ between the two groups. Of note, ablation time and total fluoroscopy time did not significantly change over time. Our data further implies that the Orion catheter is user-friendly since it can be manipulated within the atria with ease, and atrial mapping duration was reduced to  $<15$  min after a couple of procedures in experienced hands.

### Safety

The Orion catheter in conjunction with the Rhythmia system proved to be safe for LA ablation procedures. Entrapment of the basket catheter in the mitral valve apparatus was not experienced in this study. As recommended by the provider,

the mini-basket catheter was flushed with heparinized saline, and inserted to the cardiac chambers including the RA after an ACT  $>300$  s, which was maintained throughout the procedure. With these recommendations, we observed no embolic complications. In addition, all catheters were checked and found to be free from any visible thrombus formation at the end of the ablation procedure. One patient developed pericardial tamponade 3 h after the procedure, which was successfully drained from venous blood without further sequelae. As minor complications a transient air embolism ( $n = 1$ ) in the right coronary artery during pulmonary vein angiography resolving spontaneously after 6 min, and mild groin hematoma ( $n = 2$ ) were noted. As an important practical consideration, once placed in the LA, the deployed mini-basket catheter did not dislodge into the RA. Therefore, additional transseptal punctures were not necessary, which may reduce procedural risk.

### Limitations

Although this is currently the largest study reporting data from AF/AT ablation using the novel Rhythmia system, patient numbers were relatively low hampering more complex analyses, particularly in the subgroup of patients with AT. Considering a stroke risk of less than 1 % in current AF ablation procedures, procedural risk in this study may have been underestimated. Furthermore, since no information on scar was available from cardiac MRI or CT, we could not scrutinize the accuracy of the voltage maps, but this will be a topic for further research.

### Conclusions

The current study demonstrates our first clinical experience with Rhythmia, a novel high-resolution electroanatomical mapping system. Our initial data demonstrates that the combination of Rhythmia and the Orion catheter allows for a high level of acute procedural success and procedural safety for PVI and ablation of LA tachycardia. Further large-scale prospective studies with focus on LA ablation procedures including long-term follow-up data are warranted to finally determine a potential benefit for patients' treatment.

### Compliance with ethical standards

**Conflict of interest** There are no conflicts of interest.

### References

1. Camm AJ, Kirchhof P, Lip GY, Schotten U, Savelieva I, Ernst S, Van Gelder IC, Al-Attar N, Hindricks G, Prendergast B,

- Heidbuchel H, Alfieri O, Angelini A, Atar D, Colonna P, De Caterina R, De Sutter J, Goette A, Gorenek B, Haldal M, Hohloser SH, Kolh P, Le Heuzey JY, Ponikowski P, Rutten FH (2010) Guidelines for the management of atrial fibrillation: the task force for the management of atrial fibrillation of the European society of cardiology (esc). *Eur Heart J* 31:2369–2429
2. Verma A, Kilicaslan F, Pisano E, Marrouche NF, Fanelli R, Brachmann J, Geunther J, Potenza D, Martin DO, Cummings J, Burkhardt JD, Saliba W, Schweikert RA, Natale A (2005) Response of atrial fibrillation to pulmonary vein antrum isolation is directly related to resumption and delay of pulmonary vein conduction. *Circulation* 112:627–635
  3. Ouyang F, Antz M, Ernst S, Hachiya H, Mavrakis H, Deger FT, Schaumann A, Chun J, Falk P, Hennig D, Liu X, Bänsch D, Kuck KH (2005) Recovered pulmonary vein conduction as a dominant factor for recurrent atrial tachyarrhythmias after complete circular isolation of the pulmonary veins: lessons from double Lasso technique. *Circulation* 111:127–135
  4. Oakes RS, Badger TJ, Kholmovski EG, Akoum N, Burgon NS, Fish EN, Blauer JJ, Rao SN, DiBella EV, Segerson NM, Daccarett M, Windfelder J, McGann CJ, Parker D, MacLeod RS, Marrouche NF (2009) Detection and quantification of left atrial structural remodeling with delayed-enhancement magnetic resonance imaging in patients with atrial fibrillation. *Circulation* 119:1758–1767
  5. Weerasooriya R, Jaïs P, Wright M, Matsuo S, Knecht S, Nault I, Sacher F, Deplagne A, Bordachar P, Hocini M, Haïssaguerre M (2009) Catheter ablation of atrial tachycardia following atrial fibrillation ablation. *J Cardiovasc Electrophysiol* 20:833–838
  6. Jones DG, McCready JW, Kaba R, Ahsan SY, Lyne JC, Wang J, Segal OR, Markides V, Lambiase PD, Wong T, Chow AW (2011) A multi-purpose spiral high-density mapping catheter: initial clinical experience in complex atrial arrhythmias. *J Interv Card Electrophysiol* 31:225–235
  7. Nakagawa H, Ikeda A, Sharma T, Lazzara R, Jackman WM (2012) Rapid high resolution electroanatomical mapping: evaluation of a new system in a canine atrial linear lesion model. *Circ Arrhythm Electrophysiol* 5:417–424
  8. Ptaszek LM, Chalhoub F, Perna F, Beinart R, Barrett CD, Danik SB, Heist EK, Ruskin JN, Mansour M (2013) Rapid acquisition of high-resolution electroanatomical maps using a novel multi-electrode mapping system. *J Interv Card Electrophysiol* 36:233–242
  9. Anter E, Tschabrunn CM, Contreras-Valdes FM, Josephson ME (2015) Pulmonary vein isolation using the Rhythmia mapping system: verification of intracardiac signals using the Orion mini-basket catheter. *Heart Rhythm* 12:1927–1934
  10. Mantziari L, Butcher C, Kontogeorgis A, Panikker S, Roy K, Markides V, Wong T (2015) The utility of a novel rapid high-resolution mapping system in the catheter ablation of arrhythmias—an initial human experience of mapping the atria and the left ventricle. *JACC Clin Electrophysiol*. doi:10.1016/j.jacep.2015.06.002
  11. Ouyang F, Tilz R, Chun J, Schmidt B, Wissner E, Zerm T, Neven K, Köktürk B, Konstantinidou M, Metzner A, Fuernkranz A, Kuck KH (2010) Long-term results of catheter ablation in paroxysmal atrial fibrillation: lessons from a 5-year follow-up. *Circulation* 122:2368–2377
  12. Klemm HU, Steven D, Johnsen C, Ventura R, Rostock T, Lutomsky B, Risius T, Meinertz T, Willems S (2007) Catheter motion during atrial ablation due to the beating heart and respiration: impact on accuracy and spatial referencing in three-dimensional mapping. *Heart Rhythm* 4:587–592
  13. Tai CT, Liu TY, Lee PC, Lin YJ, Chang MS, Chen SA (2004) Non-contact mapping to guide radiofrequency ablation of atypical right atrial flutter. *J Am Coll Cardiol* 44:1080–1086
  14. Arentz T, von Rosenthal J, Blum T, Stockinger J, Bürkle G, Weber R, Jander N, Neumann FJ, Kalusche D (2003) Feasibility and safety of pulmonary vein isolation using a new mapping and navigation system in patients with refractory atrial fibrillation. *Circulation* 108:2484–2490
  15. Rajappan K, Baker V, Richmond L, Kistler PM, Thomas G, Redpath C, Sporton SC, Earley MJ, Harris S, Schilling RJ (2009) A randomized trial to compare atrial fibrillation ablation using a steerable vs. a non-steerable sheath. *Europace* 11:571–575
  16. Thajudeen A, Jackman WM, Stewart B, Cokic I, Nakagawa H, Shehata M, Amorn AM, Kali A, Liu E, Harlev D, Bennett N, Dharmakumar R, Chugh SS, Wang X (2015) Correlation of scar in cardiac MRI and high-resolution contact mapping of left ventricle in a chronic infarct model. *Pacing Clin Electrophysiol* 38:663–674
  17. Jadidi AS, Duncan E, Miyazaki S, Lellouche N, Shah AJ, Forclaz A, Nault I, Wright M, Rivard L, Liu X, Scherr D, Wilton SB, Sacher F, Derval N, Knecht S, Kim SJ, Hocini M, Narayan S, Haïssaguerre M, Jaïs P (2012) Functional nature of electrogram fractionation demonstrated by left atrial high-density mapping. *Circ Arrhythm Electrophysiol* 5:32–42
  18. Martirosyan M, Kiss A, Nagy-Baló E, Sándorfi G, Tint D, Edes I, Csanádi Z (2014) Learning curve in circular multipolar phased radiofrequency ablation of atrial fibrillation. *Cardiol J* 22:260–266
  19. Miller JM, Kowal RC, Swarup V, Daubert JP, Daoud EG, Day JD, Ellenbogen KA, Hummel JD, Baykaner T, Krummen DE, Narayan SM, Reddy VY, Shivkumar K, Steinberg JS, Wheelan KR (2014) Initial independent outcomes from focal impulse and rotor modulation ablation for atrial fibrillation: multicenter FIRM registry. *J Cardiovasc Electrophysiol* 25:921–929
  20. Rillig A, Lin T, Schmidt B, Feige B, Heeger C, Wegner J, Wissner E, Metzner A, Arya A, Mathew S, Wohlmuth P, Ouyang F, Kuck KH, Tilz RR (2016) Experience matters: long-term results of pulmonary vein isolation using a robotic navigation system for the treatment of paroxysmal atrial fibrillation. *Clin Res Cardiol* 105:106–116